

Improvement of photoelectrochemical HClO production under visible light irradiation by loading Cobalt oxide onto BiVO₄ photoanode

Sayuri Okunaka, Yugo Miseki, Kazuhiro Sayama

Experimental

Preparation of MO_x/FTO anode

The MO_x (where M = Co, Fe, and Ni) layer on a FTO anode (denoted as MO_x/FTO) was prepared by spin-coating (1500 rpm, 15 s) metal organic solution in butyl acetate and calcination at 400 °C for 1 h in air.

Characterization

The anode samples obtained were characterized using X-ray diffraction (XRD; PANalytical, EMPYREAN, rotating anode diffractometer, 40 kV, 10 mA) with Cu K α radiation ($\lambda_{K\alpha} = 1.5406\text{\AA}$), X-ray photoelectron spectroscopy (XPS; Ulvac Co., XPS-1800), scanning electron microscopy (SEM; HITACHI, SU8200), and UV-vis-NIR spectrometer (UV-vis. DRS, JASCO, Y-730). The CoO_x coverage was calculated using the spectrum area obtained from XPS spectrum and intensity factor of Co to the sum of those of Co, Bi, V, W and Sn.

Electrochemical performance of MO_x/FTO anode

The electrochemical performance of the MO_x/FTO anodes was measured using an electrochemical analyzer (BAS. Inc., ALS 760E). All the electrochemical performances were carried out by using a two-compartment cell (Pyrex-made) with an ion-exchange membrane (SELEMION, AGC Engineering), and an anode as the working electrode, an Ag/AgCl electrode as the reference electrode, and a Pt wire as the counter electrode. The scan rate was 50 mV s⁻¹. An aqueous solution of 0.5 M NaCl (35 mL, pH = 5.9) and 0.5 M NaClO₄ was used as the electrolyte.

Results

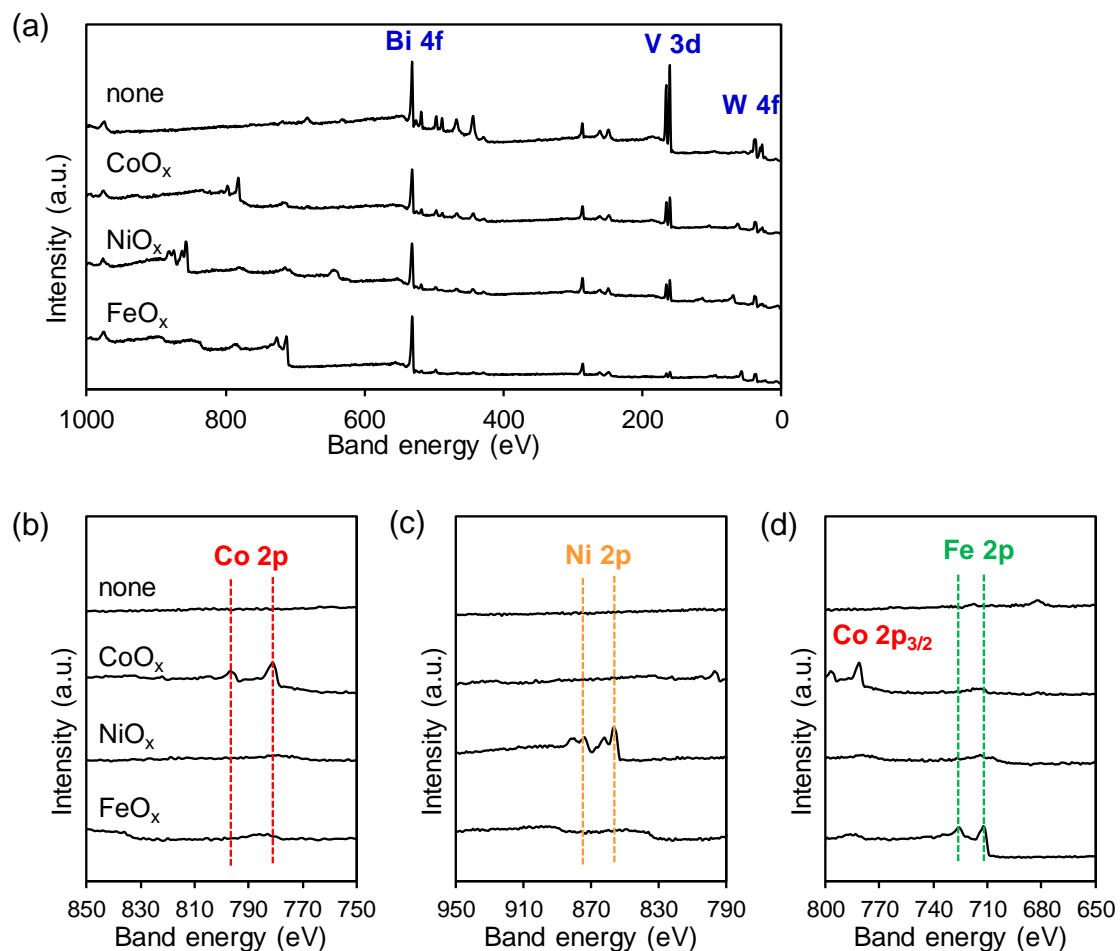


Figure S1. XPS spectra of a pristine $\text{BiVO}_4/\text{WO}_3$ photoanode and those loaded with metal oxides (MO_x ; $M = \text{Co}, \text{Ni},$ and Fe). Metal oxides were loaded by using 0.01 M of corresponding precursor metal organic solution. **(a)** wide spectrum, and narrow spectra of **(b)** Co 2p, **(c)** Ni 2p, **(d)** Fe 2p, respectively.

The spectrum of $\text{CoO}_x/\text{BiVO}_4/\text{WO}_3$ photoelectrode has two peaks at 780 and 796 eV, which are assigned to Co $2p_{3/2}$ and Co $2p_{1/2}$ in Co(III), respectively. In the spectrum of $\text{NiO}_x/\text{BiVO}_4/\text{WO}_3$ photoelectrode, two major peaks at 856 eV and 874 eV corresponding to the Ni $2p_{3/2}$ and Ni $2p_{1/2}$ in Ni(II) were appeared. In the spectrum of $\text{FeO}_x/\text{BiVO}_4/\text{WO}_3$ photoelectrode two typical peaks at 724 and 711 eV corresponding to the Fe $2p_{1/2}$ and Fe $2p_{3/2}$ spin-orbits in Fe(III) were observed.

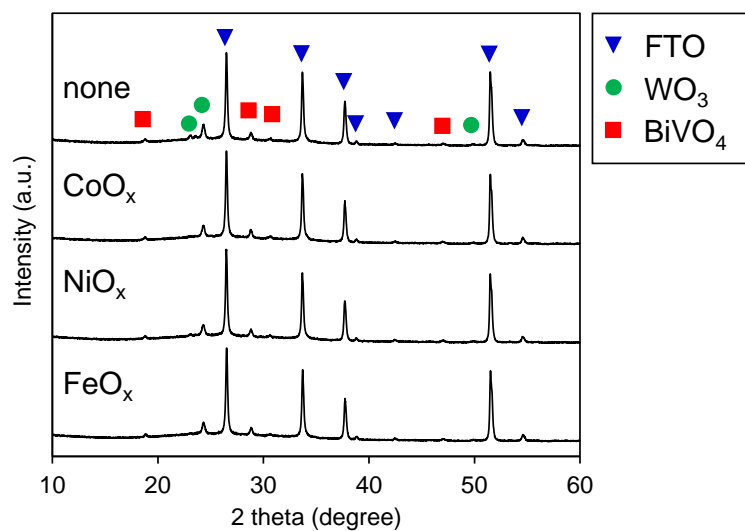


Figure S2. XRD spectra of a pristine $\text{BiVO}_4/\text{WO}_3$ photoanode and $\text{MO}_x(0.01 \text{ M})/\text{BiVO}_4/\text{WO}_3$ photoanode ($\text{M} = \text{Co}, \text{Ni}, \text{and Fe}$).

The lattice diffractions of FTO (JCPDS: 46–1088), WO_3 (JCPDS file 87-2404) and BiVO_4 (JCPDS. No. 14–0688) were confirmed. The peaks intensity of $\text{BiVO}_4/\text{WO}_3$ electrode was not weakened after loading with CoO_x .

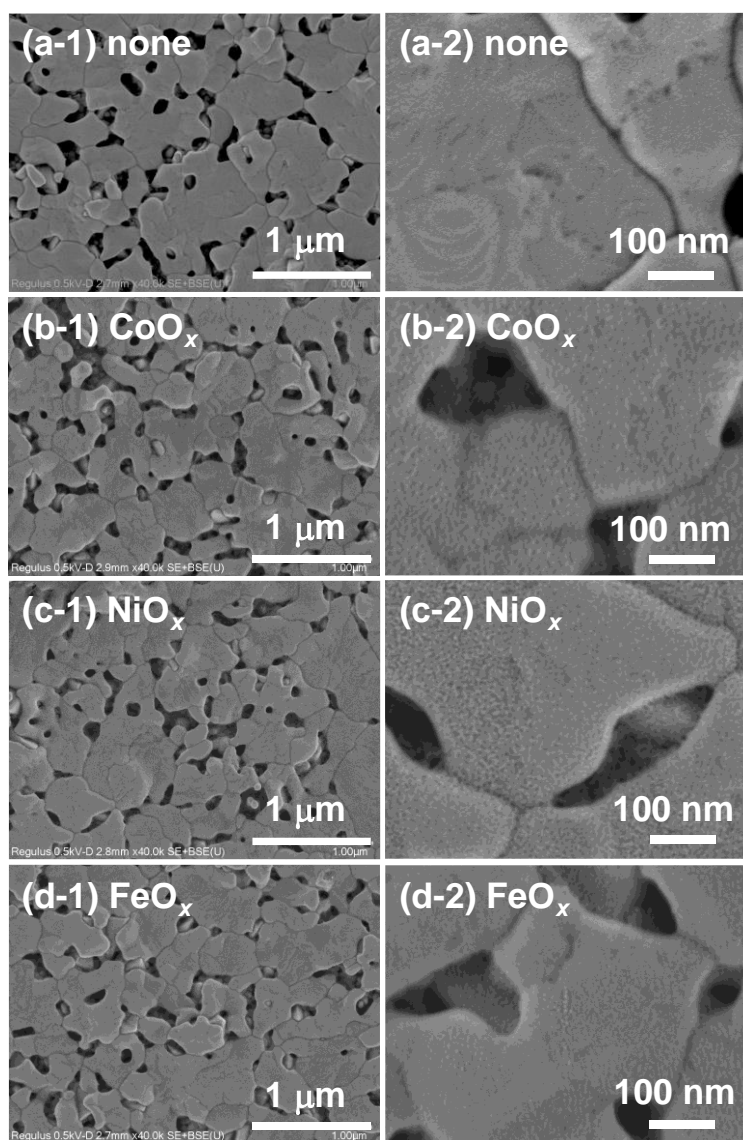


Figure S3. SEM images of a **(a)** pristine BiVO₄/WO₃ photoanode and **(b-d)** those loaded with metal oxides (MO_x; M = Co, Ni, and Fe) with low and high magnifications. The concentration of precursor solution of MO_x on the BiVO₄/WO₃ photoanodes is 0.01 M. The surface of the pristine photoelectrode appears to form small hollows. These small hollows are probably the parts where BiVO₄ was not sufficiently sintered.

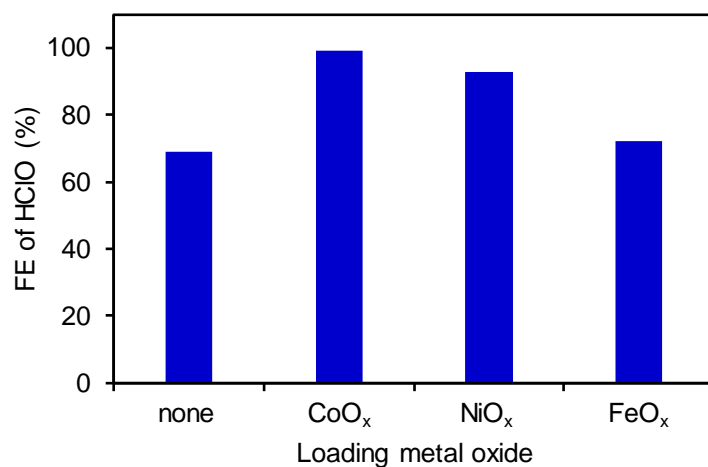


Figure S4. Faraday efficiency of HClO on the electrochemical oxidation (1 mA, 1 C) over the FTO anode with/without loading metal oxide (MO_x; M = Co, Ni, and Fe). The concentration of precursor solution of MO_x on the BiVO₄/WO₃ photoanodes is 0.01 M.

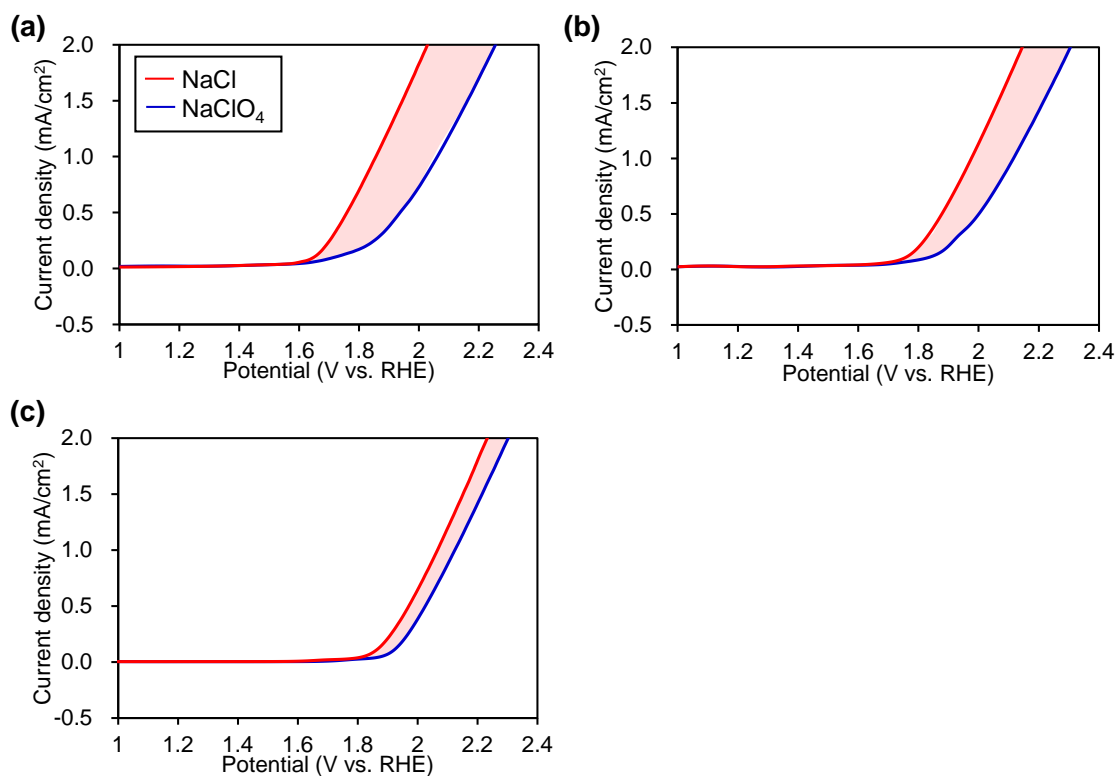


Figure S5. LSV curves for MO_x/FTO anode (M = (a) Co, (b) Ni, and (c) Fe) that were taken at 1 mV s⁻¹ in 0.5 M solution of (red) NaCl and (blue) NaClO₄ in the dark. The concentration of precursor solution of MO_x on the FTO anodes is 0.01 M.

Table S1. Amount of CoO_x loading on the $\text{BiVO}_4/\text{WO}_3/\text{FTO}$ photoanodes.

Concentration of precursor solution (M)	CoO_x loading ($\mu\text{mol}/\text{cm}^2$)
0	n.d.
0.001	n.d.
0.005	0.001
0.01	0.002
0.03	0.010
0.05	0.013
0.1	0.015

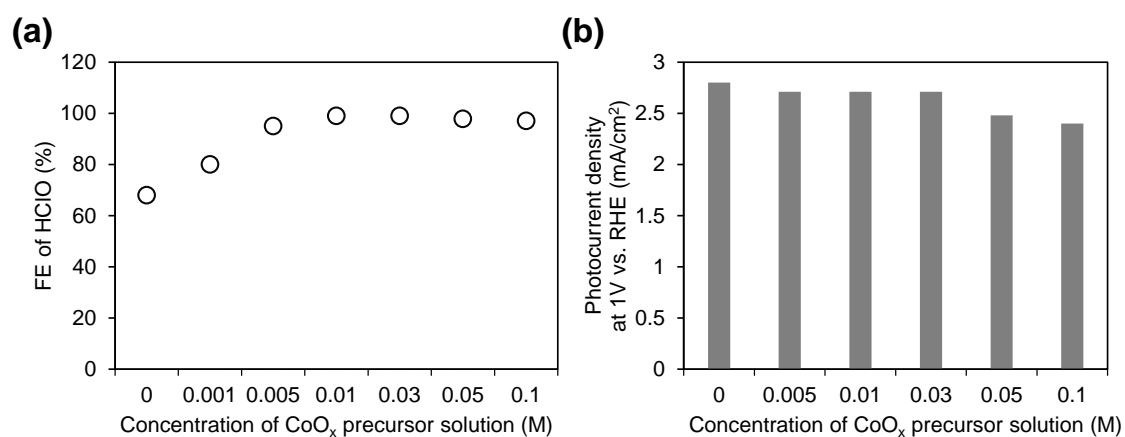


Figure S6. Effect of CoO_x loading amount on (a) FE of the HClO production and (b) photocurrent density over $\text{BiVO}_4/\text{WO}_3$ photoanode with CoO_x . Photoelectrolysis condition: 1 mA for 1000 s, Electrolyte: 0.5 M NaCl aqueous solution, light source: simulated solar light (AM 1.5) with an L-42 cut off filter, and irradiation area: *ca.* 5.0 cm^2 .

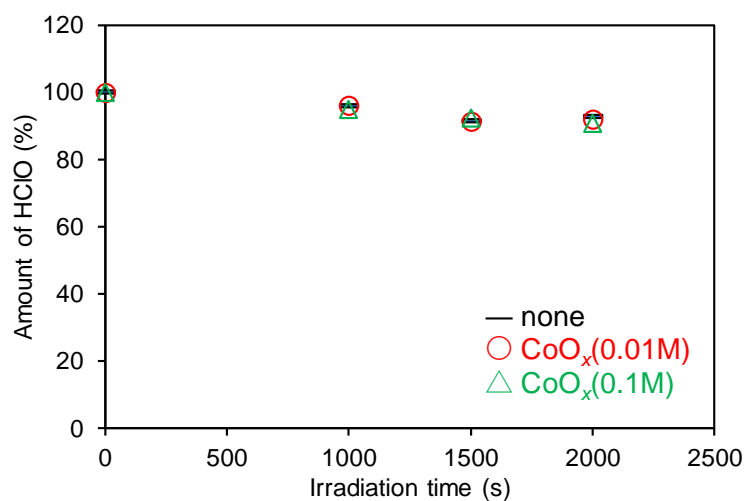


Figure S7. HClO decomposition behaviors of pristine and CoO_x modified BiVO₄/WO₃ photoanodes under solar-light irradiation. Electrolyte: 0.5 M NaCl aqueous solution, light source: simulated solar light (AM 1.5) with an L-42 cut off filter, stable current: 1 mA, and irradiation area: *ca.* 5.0 cm².

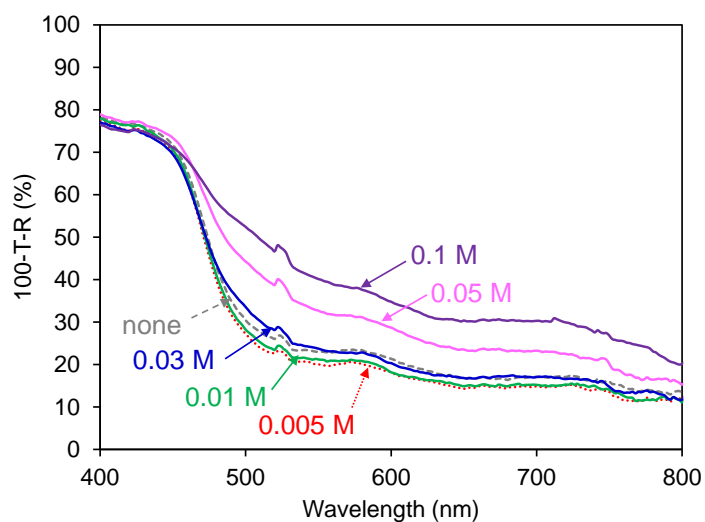


Figure S8. UV-vis spectra of BiVO₄/WO₃ photoanode modified with/without CoO_x.

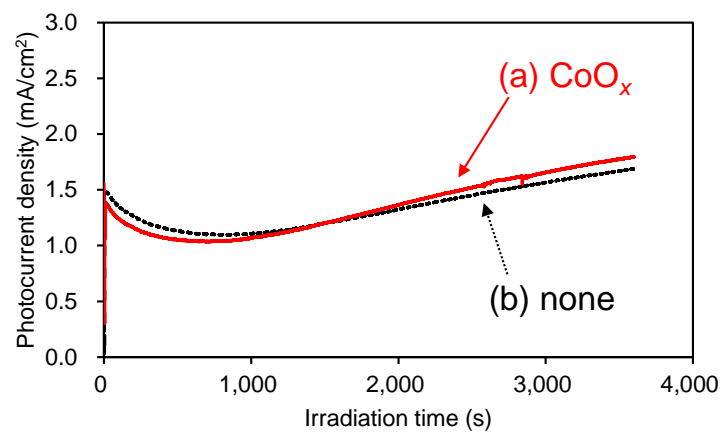


Figure S9. The amperometric $I-t$ curves of (a) $\text{CoO}_x(0.01 \text{ M})/\text{BiVO}_4/\text{WO}_3$ photoanode and (b) pristine $\text{BiVO}_4/\text{WO}_3$ photoanode under continuous illumination at 0.8 V vs. RHE. Electrolyte: 0.5 M NaCl aqueous solution, light source: simulated solar light (AM 1.5) with an L-42 cut off filter, stable current: 1 mA, and irradiation area: *ca.* 5.0 cm².